Constructing a hodoscope for the milliQan experiment: Searching for fractionally charged particles at the Large Hadron Collider

Natalie McGee
*2023 Physics REU, Department of Physics, University of California, Santa Barbara and Department of Physics, Wellesley College**

Ryan Schmitz (Graduate Mentor) and David Stuart (Faculty Mentor)
Department of Physics, University of California, Santa Barbara
(Dated: September 24, 2023)

Through a series of scintillation-based detectors at the Large Hadron Collider at CERN, the milliQan experiment will collect world-leading measurements in the search for theoretical dark matter fermions known as millicharged particles (MCPs). One such detector, the milliQan bar detector, uses 64 scintillating plastic bars aimed at an interaction point in the LHC to detect particles with a small fractional charge. The alignment of the bar detector will be performed and verified with the use of a hodoscope, which will reconstruct the paths of muons created at the interaction point. In this project we build, test, and implement changes to the hodoscope design for later use in the milliQan bar detector. We simulate beam particles with LED pulses and cosmic muons to test each step of the data acquisition and readout process, and implement the necessary improvements to the device. Finally, we propose a procedure for light-proofing the scintillator bars, mounting SiPMs, and constructing four-bar modules ("packs") which will be combined to create the layers of the hodoscope.

I. INTRODUCTION

A. Motivation

As of 2023, the Standard Model of particle physics is still the most successful understanding of the universe. Under the Standard Model, all visible matter is made up of 12 fundamental particles called fermions whose interactions are governed by 5 force carriers, or bosons [1]. Nonetheless, we know this model is incomplete, as it fails to account for several extremely well-founded observations. One of these is the existence of dark matter, the name given to the invisible particles that account for a large fraction of the mass-energy of our universe [5].

One of the most notable properties of dark matter is that it is, by definition, "dark:" dark matter has long been believed not to interact with the electromagnetic force, rendering it effectively invisible to our searches [2].

The lack of an explanation within the Standard Model has prompted investigations into a variety of Beyond-Standard-Model (BSM) explanations. One prominent family of BSM dark matter theories, known as "Dark Sector" theories, suggest that dark matter may be part of an entire set of particles, similar to—but separate from—the Standard Model itself [3]. According to these theories, dark matter would not be a single type of particle, but may include several, including various "dark fermions" and "dark bosons" (Figure 1). It is reasonable to predict that particles in the Dark Sector may interact with each other in ways analogous to the interactions within the Standard Model. The mathematics that govern SM interactions, therefore, known as group theory and quantum field theory, can be extended to this new theoretical sector [3][4].

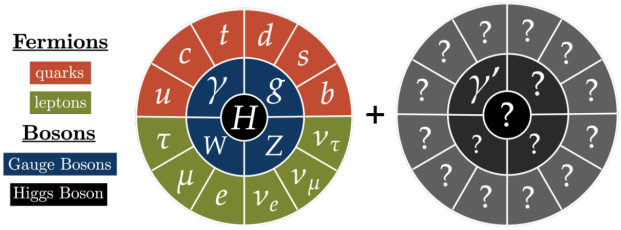

FIG. 1. Dark Sector theories propose the existence of an entire sector of dark datter particles, possibly including dark fermions and bosons, beyond the Standard Model [5].

Though we cannot predict with certainty the details of what particles and symmetry groups this Dark Sector would contain (and we cannot assume that it would mirror the Standard Model exactly), there are still some reasonable assumptions that can be made. Within the Standard Model, the simplest group is the U(1) unitary group, also known as electromagnetism. This includes only one force carrier—the photon—that interacts with only one physical property, electric charge. The two other fundamental forces within the Standard Model, SU(2) and SU(3), or the Weak and Strong nuclear forces, would be less natural additions to the Dark Sector. If there exists an invisible Dark Sector beyond the Standard Model, and it contains group symmetries governed by the same laws, it would likely include a dark analogue to electromagnetism [6].

Even this modest extension leads to some fascinating

* nm108@wellesley.edu

implications. A dark electromagnetism would necessitate the existence of a "dark photon," as well as dark fermions that interact with it through their possession of a dark charge [7]. It was this observation that led to new ideas regarding how to detect these supposedly invisible particles. In 1986, theorist Bob Holdom showed that incorporating the dark unitary group into the Standard Model Lagrangian produced a small—but significant—term in the equation that included components of both the Dark Sector and SM physics [4]. Called a kinetic mixing term, this value provides a link between dark matter and visible matter, suggesting that any dark matter fermion with a dark charge would be able to couple not only with a dark photon, but also with a SM photon. In other words, dark matter fermions would appear to have a regular, electric charge, just like a SM fermion might. The strength of this SM coupling is proportional to the term ke', where k is the kinetic mixing strength and e' is the fundamental dark charge (as opposed to e, the fundamental SM electron charge). However, the value of k is expected to be very small: likely on the order of 10^{-3}. This means that though dark fermions couple with visible photons, their coupling strength is weak. To us, this would look like a particle with an extremely small charge: a millicharged particle (MCP).

As a consequence, dark matter, rather than being truly "dark" or invisible, could in fact just be very, very "dim." We could be able to detect it using some of the same techniques we use to detect SM particles, namely by observing its interactions with electromagnetism. At the same time, its small charge would explain why it has yet to be detected. The energy deposited by a charged particle in a detector is typically proportional to the square of its charge. As a result, existing particle detectors, designed almost exclusively to detect particles with an electron charge or more, are not sensitive to MCPs [5]. MCPs could be prevalent but existing experiments are unable to see them.

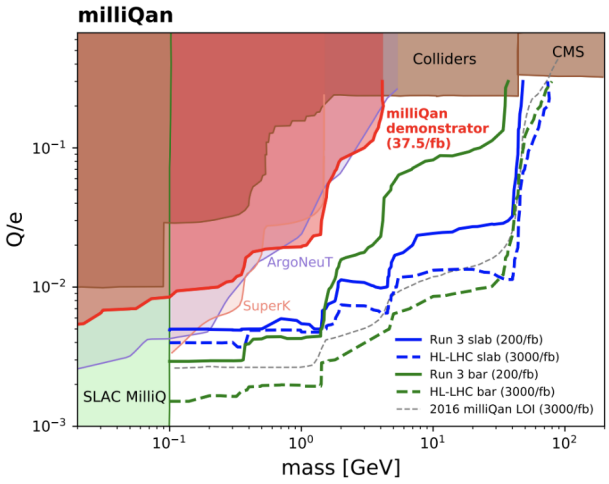

FIG. 2. The parameter space of plausible characteristics of the theoretical MCPs and the sensitivities of different detectors. The milliQan demonstrator (shaded red) and Bar and Slab detectors (solid green and blue) will be world-leading in searching for fractionally charged particles between 10^{-1} and 10^{2} GeV [8].

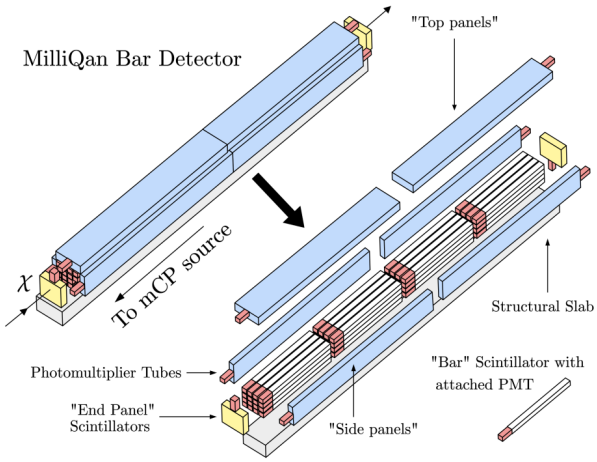

FIG. 3. A diagram of the MilliQan bar detector and its components. The bar detector consists primarily of 64 scintillator bars arranged in four layers placed end-to-end [9].

B. MilliQan Bar Detector

The milliQan experiment is specifically designed to detect particles with millicharge, allowing investigation into phenomena that would be invisible to other experiments (Figure 2). MilliQan encompasses several devices in various phases of production and implementation, all of which use the particle-detecting capabilities of scintillators to search for MCPs.

One such device, the millQan Bar Detector, is located at the Large Hadron Collider (LHC) at CERN in Switzerland. The milliQan Bar detector is constructed of 64 5x5x60 cm bars of scintillating plastic arranged in 4 layers of 16 bars, with the layers placed end-to-end (Figure 3). Each bar has a photomultiplier tube (PMT), a type of light detector capable of sensing individual photons created in the scintillator, fastened to one end. The detector also has panels of scintillating material positioned on either end and along the sides, primarily useful for identifying non-MCP background particles. As a charged particle travels up the detector, it will hit at least one bar in each layer, creating a trail of photons and a series of time- and location-dependent signals (Figure 4).

The number of photons generated by a single through-going particle is proportional to the square of the particle's charge, and to the length of the path the particle takes through the scintillating material [11]. Because of their small charge, MCPs would be capable of traversing a piece of scintillating material and only producing very few photons, or none at all. The design of the milliQan bar detector accounts for this by using long bars aligned

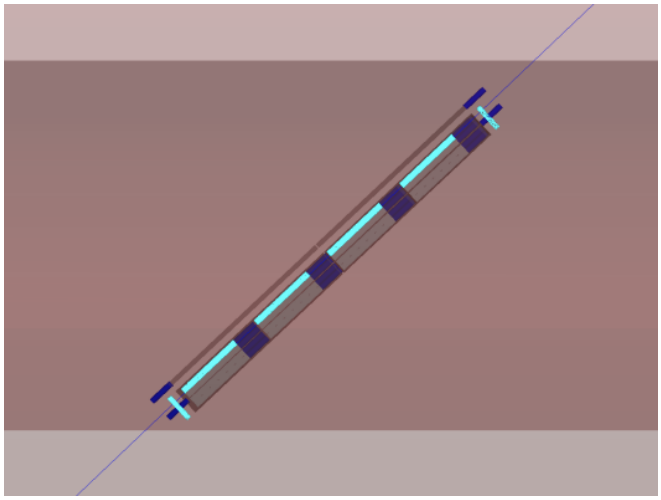

FIG. 4. Output of a GEANT4 simulation showing a MCP with charge q=0.004e traversing the length of the bar detector [10].

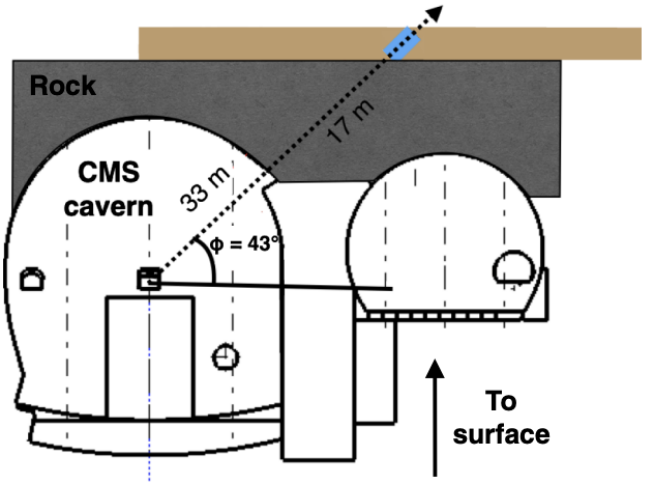

FIG. 5. The bar detector is located at the LHC in a tunnel crossing above the CMS detector. The bar detector is 33m away from the IP, pointed downwards at an angle aligned with the path of particles produced in the collisions [5].

along the particle's path, rather than by using shorter bars or panels, thus maximizing the distance the particles travel through the scintillators and increasing the likelihood that a MCP would generate enough photons to create a clear signal [7]. The bars used by the milliQan bar detector are 60 cm in length. For comparison, the detectors used by the Compact Muon Solenoid experiment (CMS) at the Large Hadron Collider (LHC) have a thickness on the order of 100 microns [12].

The bar detector records the amplitude (proportional to the number of photons detected within a bar), time, and location of each PMT signal it receives. From this information, the path of the particle, along with its velocity and charge, can be estimated.

The bar detector itself is located in a drainage gallery (a narrow, concrete tunnel) positioned above the CMS experiment in the LHC. The Interaction Point (IP) where the proton-proton collisions occur is 33 meters below the bar detector, 17 meters of which is solid rock (Figure 5). Unwanted particles, such as protons and electrons, would be stopped by this barrier. However, MCPs produced in the same collisions would be more than capable of traversing it thanks to their weak ionization strength.

C. The Hodoscope

The purpose of the hodoscope is to aid in aligning the bar detector by pointing it at the IP. A precisely aligned detector enables more effective measurements of the path, charge, and velocity of the particles that pass through it. If the detector is misaligned, particles may not travel up along its length, but rather cross through at an angle, generating fewer signals and making their properties more difficult, or impossible, to identify.

The detector is currently aligned using a laser survey conducted by CERN, which claims a precision to approximately 1 cm from the IP [10]. However, this measurement is several years old, a time period during which the detector has been significantly repaired, adjusted, etc. Thus, a secondary system of alignment was proposed in the form of a hodoscope.

The hodoscope, from the Greek prefix hodo- meaning "path," tracks the path of certain particles. For this purpose, the hodoscope will detect muons, which (like MCPs) are also created in the proton-proton collisions in the LHC. Muons are the only charged SM particles capable of traversing the 17 m of rock, and possess a full electron charge, making them much easier to detect than MCPs. The hodoscope will consist of several detection layers at the front and end of the bar detector, each of which will record the x- and y-coordinate of a through-going particle. Using these points, the muon angular distribution can be used to extrapolate the detector's alignment with the IP.

The hodoscope will complement the existing survey-based alignment system by providing a simple, noninvasive mechanism for determining the alignment of the detector, and can be operated as frequently as necessary to provide certainty.

II. HODOSCOPE DESIGN

The hodoscope consists of several modules that can be layered and placed around the bar detector as necessary (Figure 6). Each module contains two layers of 16 parallel scintillator bars, 1.5x1.5x24 cm in size, with the bars in one layer oriented perpendicular to the other [13]. Each bar will have a silicon photomultiplier (SiPM), a type of

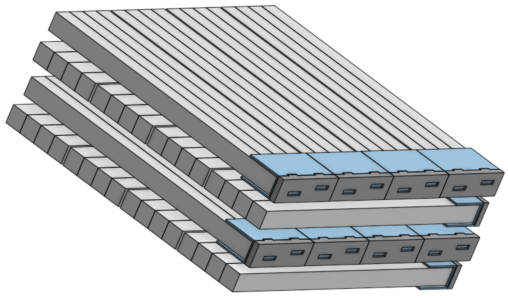

FIG. 6. The hodoscope is made of layers of 16 parallel scintillator bars arranged in 4 packs of 4 bars. The layers are crossed to provide x- and y-coordinates of a through-going muon.

small photodetector, mounted to the end. To prevent cross-talk from escaped photons, the bars will be light-proofed using layers of paper and electrical tape. As a muon passes through the layers of the hodoscope, it will activate one bar in each layer, providing x- and y-location information as well as a timestamp.

The 16 bars in each layer are divided into 4 packs of 4 bars. Each pack is mounted to a circuit board containing 4 SiPMs. The time-varying current signals produced by each SiPM are converted to voltages, amplified, then translated to a digital signal. The digital outputs are then processed by a large readout board that collects signals from all 4 packs with a Raspberry Pi Pico. The Pico converts the digital signals to numerical data for later, remote processing.

A. Detection Mechanisms

The hodoscope makes use of an array of scintillating plastic bars to detect charged particles. When a through-going charged particle ionizes an atom within the scintillating material, the atom recombines with an electron at a higher energy level. It then returns to its ground state, releasing a photon [11]. The resulting trail of photons left in the scintillating bar scatters in all directions. A portion of them are absorbed by the SiPM mounted on the end of the bar.

The SiPM is a type of photodetector that outputs a time-varying current signal proportional to the number of photons it absorbs. Its structure is similar to that of a typical photodiode, which generates current by absorbing photons. However, unlike simple photodiode light detectors, a SiPM is made of diodes that are held at a very high reverse bias. This bias voltage is close enough to the diode's breakdown voltage that the absorption of a single photon causes the diode to break down, triggering an avalanche that releases a large amount of current. The result of a SiPM absorbing a photon is similar to closing a switch in a RC circuit and allowing a capacitor to discharge. In this way, the SIPM is capable of amplifying a very small signal from a single photon to a time-varying current that is large enough to be processed.

The SiPMs used in the hodoscope are 3mmx3mm squares [14], and thus do not cover the entire end of each bar. As a result they do not capture every photon that is created, but we expect a through-going muon to generate enough photons that even collecting a fraction of the light should still be a sufficiently large signal. SiPMs are also less sensitive than photomultiplier tubes (PMTs), the photodetectors used in the milliQan bar detector. However, they are much more compact and durable and less expensive. Unlike the bar detector, the hodoscope does not need to be sensitive to individual photons, making SiPMs the appropriate choice.

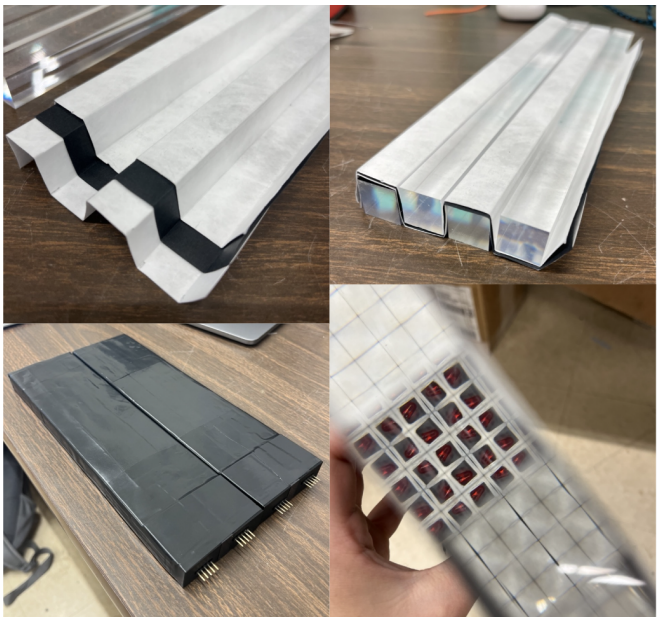

FIG. 7. Steps in the process of constructing a hodoscope pack. Clockwise from top left: Alternating sheets of folded white and black paper, pulled apart to show lower layers. Four scintillator bars wrapped in paper. A view down the length of a bar with a single red LED on the opposite end, demonstrating the reflective properties of the bar. Two completed hodoscope packs.

B. Hodoscope Packs

Each layer of the hodoscope consists of four packs of four scintillator bars placed side by side. The bars are 1.5x1.5x24 cm in size. To prevent photons from crossing between bars, they are wrapped in three layers of white and black paper (Figure 7). Most photons created within the bars will travel along the length of the bar as a result of total internal reflection, though some will be created at too steep of an angle to be reflected. These photons will ideally be reflected back into the bar by the white paper, or at the very least absorbed by one of the three layers. Additionally, a strip of reflective material [15] is

placed at the far end of each pack to reflect back any photons traveling away from the SiPM. The pack is then wrapped in black electrical tape to prevent external light from entering the bars.

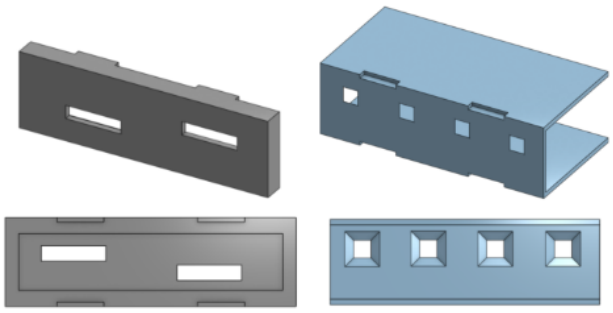

FIG. 8. CAD model for SiPM mount and cap. Back views are shown below angled views. The SiPM board is placed in the recessed area of the cap (gray). Note the chamfered edges of the square holes in the mount (blue), which are designed to improve light collection efficiency (Figure 13).

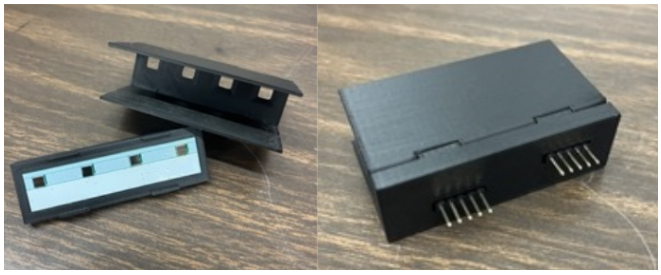

FIG. 9. A populated SiPM board placed in the mount cap and a view of the fully assembled SiPM mount.

Each bar has a SiPM mounted to the open end. The four SiPMs in each pack are attached to a single PCB with two 5-pin headers that connects the SiPMs to the readout electronics. This SiPM board attaches to the hodoscope pack with a 3D printed mount made of two parts. The primary mount is fixed semi-permanently to the end of the hodoscope pack, while the SiPM board itself is in a seperate "cap" that can be attached and detached from the mount (Figures 8, 9). This design provides some physical protection to both the hodoscope bars and the SiPMs and allows for relatively easy assembly and disassembly in case the SiPMs need to be serviced. It also reduces light leaks while ensuring most efficient light collection. Full technical drawings of the SiPM mounts can be found in Appendix B: Technical Drawings.

To form a layer, four completed packs will be wrapped together with electrical tape and readout electronics will be added to the end of each pack.

C. Electronics

The time-varying current signals from the SiPMs are processed with a series of small PCBs that convert the current to a voltage, amplify the signal, and compare it to a threshold voltage to convert the pulse to single-bit digital data. Each pack of four bars is mounted to a single SiPM board and possesses its own amplifier board and digital board. A single large readout board will connect the four packs in a layer to each other and to a Raspberry Pi Pico. Detailed schematics for each board can be found in Appendix A: Schematics.

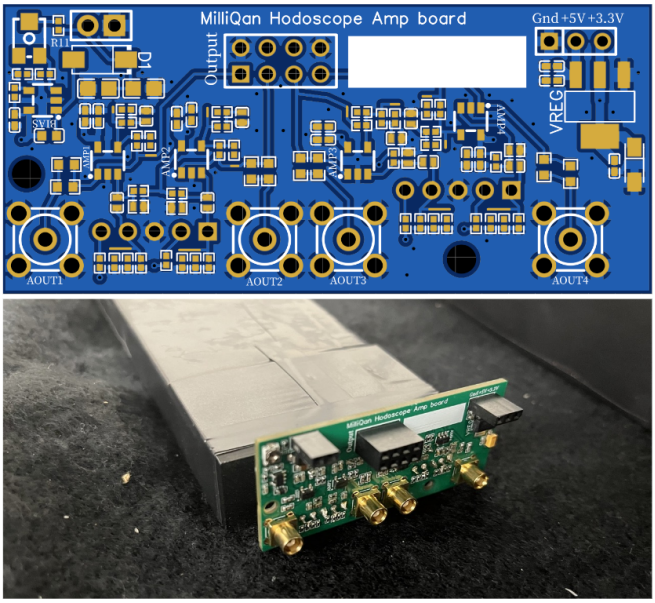

FIG. 10. A computer model of the amplifier board and a view of the board connected to a hodoscope pack. The amplifier board converts the signals from 4 SiPMs to amplified voltage outputs. For full schematics, see Appendix A: Schematics

The amplifier board (Figure 10) receives the time-varying current signals from the SiPMs, converts them to time-varying voltages, and amplifies the signals. There are four separate op-amp non-inverting amplifier circuits, one for each channel. The amplified output can then be read out two ways: either with the MCX connectors along the bottom of the board or with the 8-pin connector at the top. The 8-pin connector outputs are designed to send the amplified signals to the digital board. The amplifier board is also responsible for generating the bias voltage that is used to power the SiPMs. The value of the bias voltage is set universally for the 4 SiPMs connected to the board using a potentiometer. As of the writing of this paper, some changes are being implemented into the amplifier board schematic. See Appendix A for more information.

The digital board (Figure 11) receives the four analog signals from the amplifier board and converts them to time-varying digital pulses. Each signal is sent through a separate comparator circuit which outputs a high (3.3V)

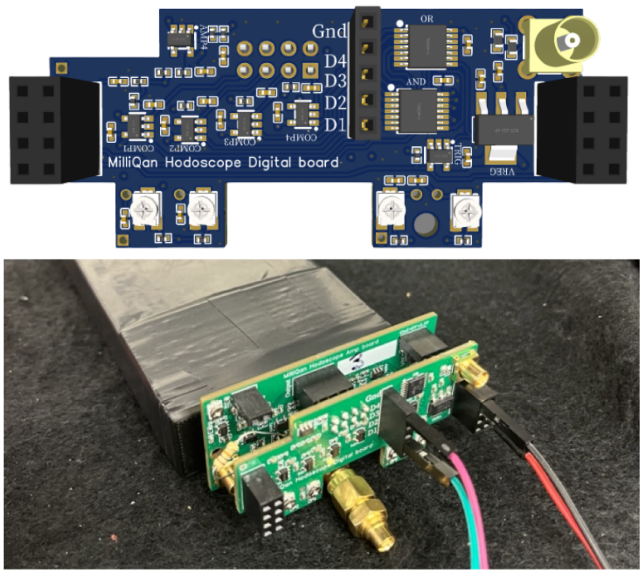

FIG. 11. A computer model of the digital board and a view of the board connected to a hodoscope pack and amplifier board. The digital board converts the amplified analog signals to digital outputs. For full schematics, see Appendix A: Schematics

logical pulse for the length of time the analog signal is above a given threshold voltage. The threshold voltage is set separately for each comparator with potentiometers. The digital signal from each channel is then sent to the readout board for processing. The digital board also performs a small amount of logic on the digital signals with logical AND and OR integrated circuits. Certain logical outputs are sent to neighboring digital boards through two 8-pin headers located on either side of the board.

The readout board (Figure 12) connects four hodoscope packs together, forming a cohesive layer. It receives 4 digital signals each from all 4 digital boards and connects these inputs to pins on a Raspberry Pi Pico. It also forms the logical connections between boards. Some logical signals, including OR outputs for each board and a global trigger signal, are sent to separate pins on the Pico to allow for logic triggering if desired. Note that the readout boards are still in production and have not been tested as of the writing of this paper. Because of this, Pico testing is being performed by connecting the Pico directly to the digital boards with jumper wires.

III. DATA ANALYSIS

Digital signals sent to the Pico are processed using a micropython script that makes use of the Pico's Programmable Input/Output (PIO) capabilities. PIO is a unique feature of the Pico that allows for the creation of custom I/O hardware logic for applications that require efficient processing. It provides dedicated state machines that can be programmed with a limited vocabulary of commands to perform tasks independently of the Central Processing Unit of the Pico.

The high efficiency of PIO programs allows the Pico to measure short pulse widths. The full code used to record pulse widths from a Pico can be found in Appendix C: Scripts and Data Analysis, and is structured as follows.

The PIO script triggers on the rising edge of a designated trigger pin, usually a logical OR or AND of several channels. Once the script has been triggered, the PIO will record the values of all 32 GPIO pins on the Pico at 8 evenly spaced time intervals. The time intervals are set by the program itself, which designates a frequency with which the commands are executed. This frequency can be up to 125 MHz. However, the FIFOs used for storing data can only record 8 32-bit words per event. Because the digital signals from the hodoscope range from 500 ns to 4000 ns in width, I selected a 10 MHz frequency, which should provide 400 ns resolution for pulse widths up to 3200 ns.

As soon as data begins to be stored in the FIFOs, a second section of the script begins emptying the FIFOs and saving the 32-bit words as binary values. These values are then saved to a CSV file along with timestamps and an event number for later processing. The current script saves the CSV file on the Pico itself, though it could be modified to save to an SD card or another computer.

To analyze this data, I prepared another script that sorts the binary values in the CSV into events and pin numbers, providing a more accessible interface with the data. The analysis script allows a user to identify which pins are of interest and can sort events for multi-pin coincidence and identify long pulses. It can also be easily modified to apply cuts on length, coincidence, and more. The full script can be found in Appendix C: Scripts and Data Analysis.

IV. DEVELOPMENT AND TESTING

The development and testing process began with using scintillator bars and SiPMs to characterize their behavior before progressing to readout electronics and troubleshooting. This involved using pre-fabricated Hamamatsu SiPM modules, which provide a reliable and sensitive SiPM response. These modules were then used to test the larger, less expensive, and less sensitive SiPMs to be used in the hodoscope. Tests included recording coincident pulses on multiple scintillator bars to measure cosmic muons and flashing LEDs for brief periods to provide a consistent and reliable photon source. LED testing was used to determine the light collection efficiency of different SiPM mount designs by comparing the average pulse size for different mounts (Figure 13)

Testing of readout electronics also began with outside components. Cosmic Catcher single-channel amplifier boards and LED readouts were modified and improved for use with a hodoscope pack to test the new SiPMs.

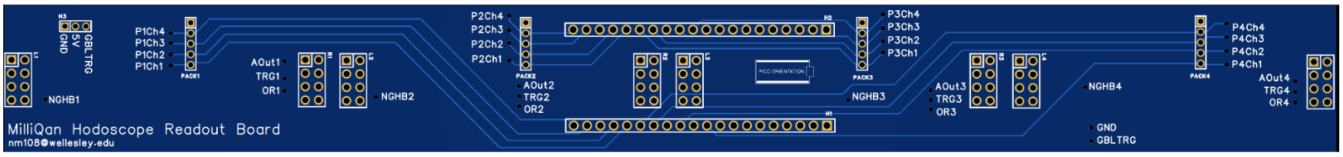

FIG. 12. A computer model of the readout board. The readout board connects all 4 packs in a layer together and sends the 16 digital signals to pins on a Raspberry Pi Pico, which will be mounted on the surface of the board. For full schematics, see Appendix A: Schematics

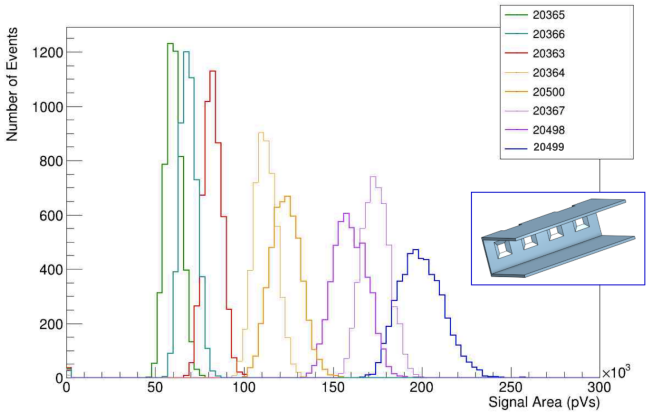

FIG. 13. Tests of several SiPM mounts were performed by flashing an LED for brief intervals at the end of a hodoscope bar. The area of pulses generated by each SiPM is shown here. Some designs proved to be more efficient at collecting photons than others, as demonstrated by a larger average pulse area. The most effective design is shown in the inset. Note the chamfered edges of the SiPM windows on this design (Run 20499, dark blue), which can be seen to improve light collection efficiency compared to the same design without chamfered windows (Runs 20500 and 20364, yellow).

They also provided a comparison for testing the next generation of 4-channel hodoscope amplifier boards.

These 4-channel amplifier boards required significant troubleshooting to create useful voltage outputs. This involved adding and removing resistors and other components to and from the board to adjust the signal output. Particularly complicated tasks included amplifying the signal enough to receive a measurable pulse, minimizing overwhelming noise signals, and adjusting pulse widths to a reasonable length. The current design (Appendix A: Schematics) appears to be satisfactory at creating large pulses in response to photon deposits, though the long decay times may cause problems from pileup of consecutive events.

The amplifier boards provide MCX ports for direct readout of the analog signals created on each channel, which I viewed on the DRS to track the board's outputs.

The digital board was more straightforward and required almost no major adjustments. To test the digital outputs, I used a function generator to create pulses of varying sizes and ensured that the digital output matched the expected values.

The function generator was also used to test the pulse measurement capabilities of the Pico by providing pulses of known widths. Initial attempts to measure these pulses used interrupts in micropython, but this process proved too slow. Once PIO capabilities were implemented, functional SiPMs, amplifier boards, and digital boards were connected directly to the Pico to test the measurement of many pins at once.

Once the functionality of multiple bars in different packs was confirmed, I was able to begin path-tracking experiments with layers of crossed and parallel bars. These provided an end-to-end proof of concept for the hodoscope and formed the foundation for larger-scale implementation.

V. DISCUSSION/FUTURE STEPS

This summer I made significant progress in designing, building, and troubleshooting the hodoscope, ultimately constructing an operational prototype. In the meantime, hodoscope packs can be used for cosmic path tracking in local applications, including the calibration of milliQan slab detectors.

I will also assemble a procedure for the construction, testing, and troubleshooting of the hodoscope according to my progress this summer. This resource will allow future students to continue my work on the hodoscope, make improvements, and ultimately guide its implementation into the milliQan bar detector in the LHC.

VI. ACKNOWLEDGEMENTS

I would like to thank my graduate mentor Ryan Schmitz and my faculty mentor David Stuart for their support throughout this project. Their eagerness to answer questions and explain problems was incredibly valuable. Thank you to all members of the Stuart lab who provided encouragement and advice, creating a welcoming environment for learning, experimentation, and problem-solving. Special thanks to Sathya Guruswamy for organizing the UCSB Physics REU and the NSF grant PHY-1852574 for funding it. Finally, I want to thank the seven other students in the REU, without whom this experience would never have been the same.

[1] CERN, The standard model (2023).

[2] CERN, Dark matter (2023).

[3] R. Essig, J. A. Jaros, W. Wester, P. H. Adrian, S. Andreas, T. Averett, O. Baker, B. Batell, M. Battaglieri, J. Beacham, T. Beranek, J. D. Bjorken, F. Bossi, J. R. Boyce, G. D. Cates, A. Celentano, A. S. Chou, R. Cowan, F. Curciarello, H. Davoudiasl, P. deNiverville, R. D. Vita, A. Denig, R. Dharmapalan, B. Dongwi, B. Döbrich, B. Echenard, D. Espriu, S. Fegan, P. Fisher, G. B. Franklin, A. Gasparian, Y. Gershtein, M. Graham, P. W. Graham, A. Haas, A. Hatzikoutelis, M. Holtrop, I. Irastorza, E. Izaguirre, J. Jaeckel, Y. Kahn, N. Kalantarians, M. Kohl, G. Krnjaic, V. Kubarovsky, H.-S. Lee, A. Lindner, A. Lobanov, W. J. Marciano, D. J. E. Marsh, T. Maruyama, D. McKeen, H. Merkel, K. Moffeit, P. Monaghan, G. Mueller, T. K. Nelson, G. R. Neil, M. Oriunno, Z. Pavlovic, S. K. Phillips, M. J. Pivovaroff, R. Poltis, M. Pospelov, S. Rajendran, J. Redondo, A. Ringwald, A. Ritz, J. Ruz, K. Saenboonruang, P. Schuster, M. Shinn, T. R. Slatyer, J. H. Steffen, S. Stepanyan, D. B. Tanner, J. Thaler, M. E. Tobar, N. Toro, A. Upadye, R. V. de Water, B. Vlahovic, J. K. Vogel, D. Walker, A. Weltman, B. Wojtsekhowski, S. Zhang, and K. Zioutas, Dark sectors and new, light, weakly-coupled particles (2013), arXiv:1311.0029 [hep-ph].

[4] B. Holdom, Two u(1)'s and charge shifts, Physics Letters B **166**, 196 (1986).

[5] A. Ball, G. Beauregard, J. Brooke, C. Campagnari, M. Carrigan, M. Citron, J. De La Haye, A. De Roeck, Y. Elskens, R. E. Franco, M. Ezeldine, B. Francis, M. Gastal, M. Ghimire, J. Goldstein, F. Golf, J. Guiang, A. Haas, R. Heller, C. S. Hill, L. Lavezzo, R. Loos, S. Lowette, G. Magill, B. Manley, B. Marsh, D. W. Miller, B. Odegard, F. R. Saab, J. Sahili, R. Schmitz, F. Setti, H. Shakeshaft, D. Stuart, M. Swiatlowski, J. Yoo, H. Zaraket, and H. Zheng, Search for millicharged particles in proton-proton collisions at $\sqrt{s} = 13$ TeV, Phys. Rev. D **102**, 032002 (2020).

[6] A. Haas, C. S. Hill, E. Izaguirre, and I. Yavin, Looking for milli-charged particles with a new experiment at the lhc, Physics Letters B **746**, 117 (2015).

[7] A. Ball, J. Brooke, C. Campagnari, A. D. Roeck, B. Francis, M. Gastal, F. Golf, J. Goldstein, A. Haas, C. S. Hill, E. Izaguirre, B. Kaplan, G. Magill, B. Marsh, D. Miller, T. Prins, H. Shakeshaft, D. Stuart, M. Swiatlowski, and I. Yavin, A letter of intent to install a milli-charged particle detector at lhc p5 (2016), arXiv:1607.04669 [physics.ins-det].

[8] A. Ball, J. Brooke, C. Campagnari, M. Carrigan, M. Citron, A. De Roeck, M. Ezeldine, B. Francis, M. Gastal, M. Ghimire, J. Goldstein, F. Golf, A. Haas, R. Heller, C. S. Hill, L. Lavezzo, R. Loos, S. Lowette, B. Manley, B. Marsh, D. W. Miller, B. Odegard, R. Schmitz, F. Setti, H. Shakeshaft, D. Stuart, M. Swiatlowski, J. Yoo, and H. Zaraket, Sensitivity to millicharged particles in future proton-proton collisions at the lhc with the milliqan detector, Phys. Rev. D **104**, 032002 (2021).

[9] S. D. Alcott, Development of the milliqan bar detector: a search for millicharged particles (2023), unpublished thesis.

[10] C. Hill, *Technical Proposal for the milliQan sub-detector*, Tech. Rep. (CERN, Geneva, 2021).

[11] C. Grupen, Physics of particle detection, AIP Conference Proceedings **536**, 3 (2000), https://pubs.aip.org/aip/acp/article-pdf/536/1/3/11954081/3_1_online.pdf.

[12] CERN, CMS Detector (2023).

[13] The scintillator is EJ-200 from Eljen Technology.

[14] The SiPMs used are Broadcom part number AFBR-S4K33C01XXL.

[15] The specular reflective material used is 3M part number DF2000MA.

[16] CERN, Cosmic rays: particles from outer space (2023).

Appendix A: Schematics

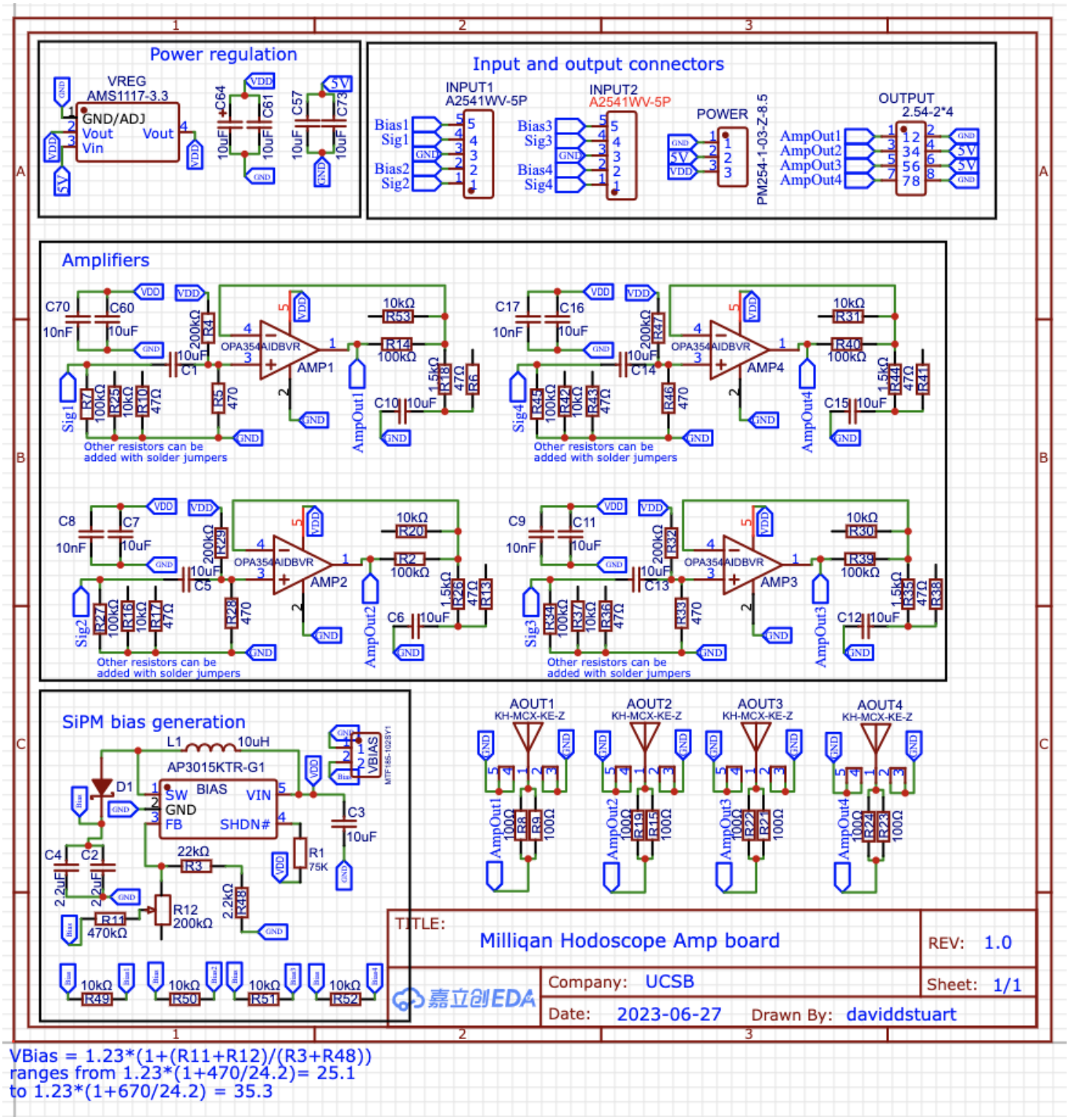

FIG. 14. Schematic of Amplifier Board. As of the writing of this paper, some changes are being made to this design. Pending the results of further testing, these changes will be implemented in later generations of the amplifier board. One recent attempt replaces 470 Ω resistors R5, R46, R28, and R33 with 10 kΩ resistors. Resistors R6, R41, R13, and R38, as well as R10, R46, R17, and R33 are connected using solder jumpers. The most recent iteration simply replaces R5, R46, R28, and R33 with 2 kΩ resistors. This iteration appears the most promising.

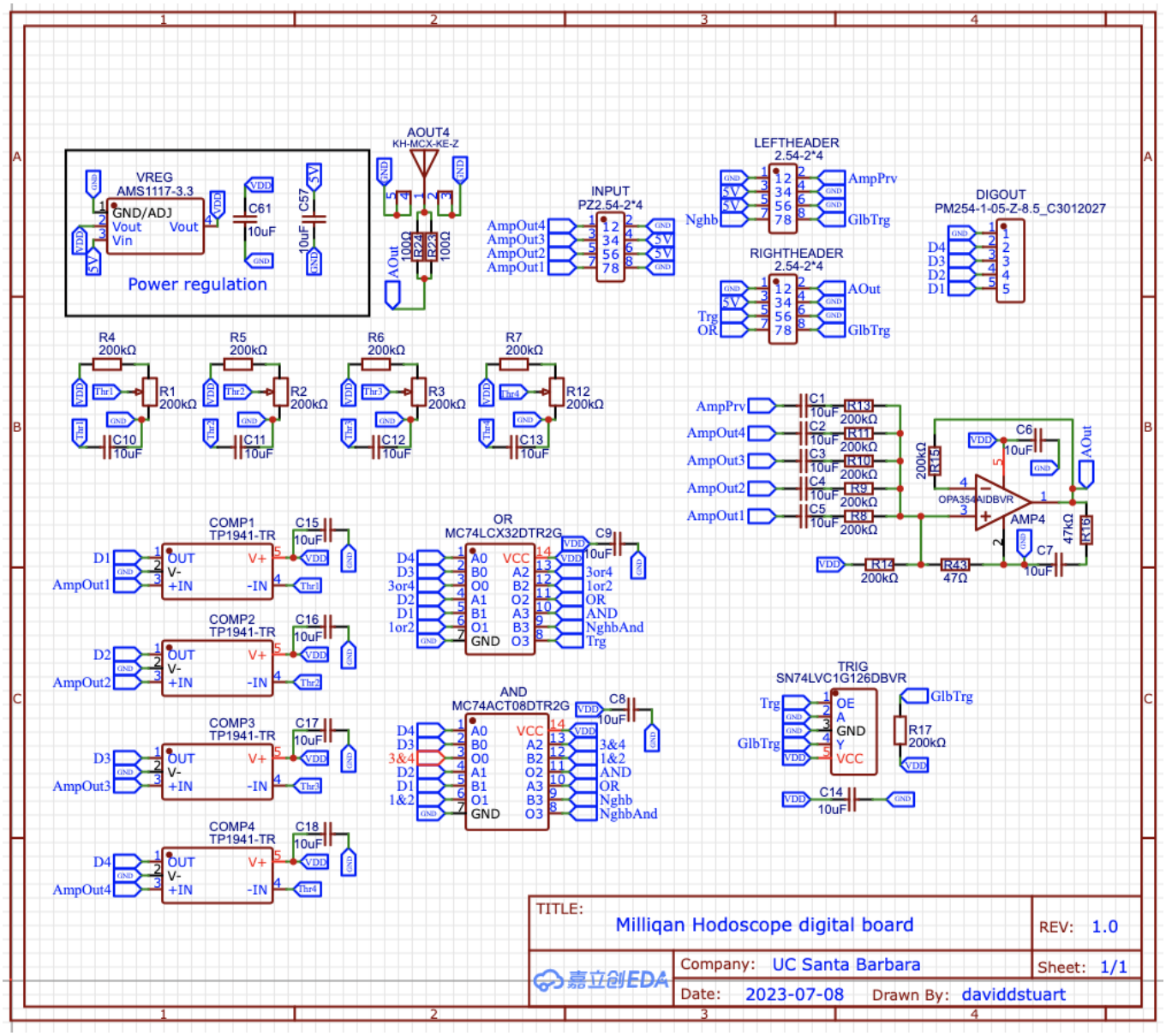

FIG. 15. Schematic of Digital Board

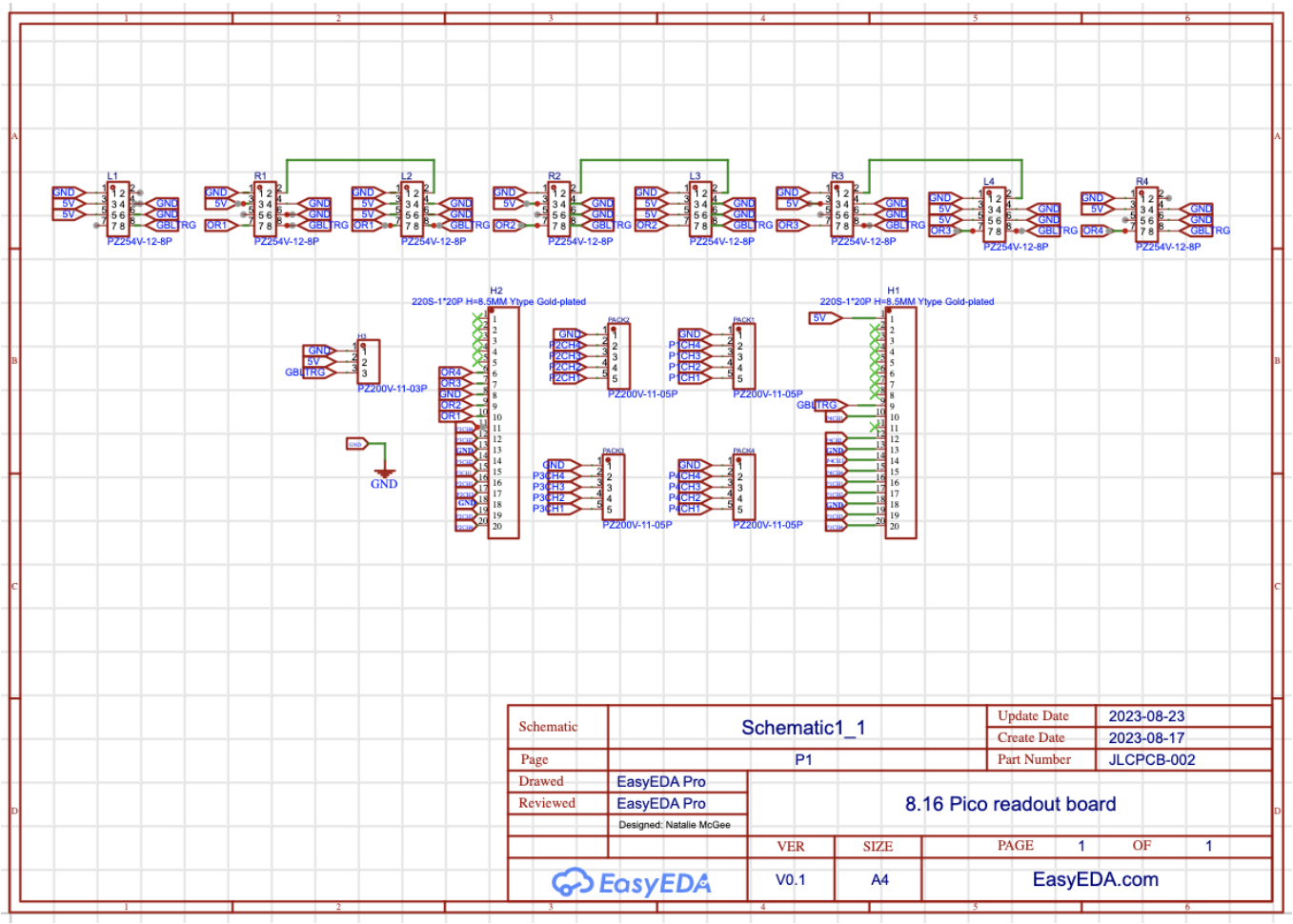

FIG. 16. Schematic of Readout Board.

Appendix B: Technical Drawings

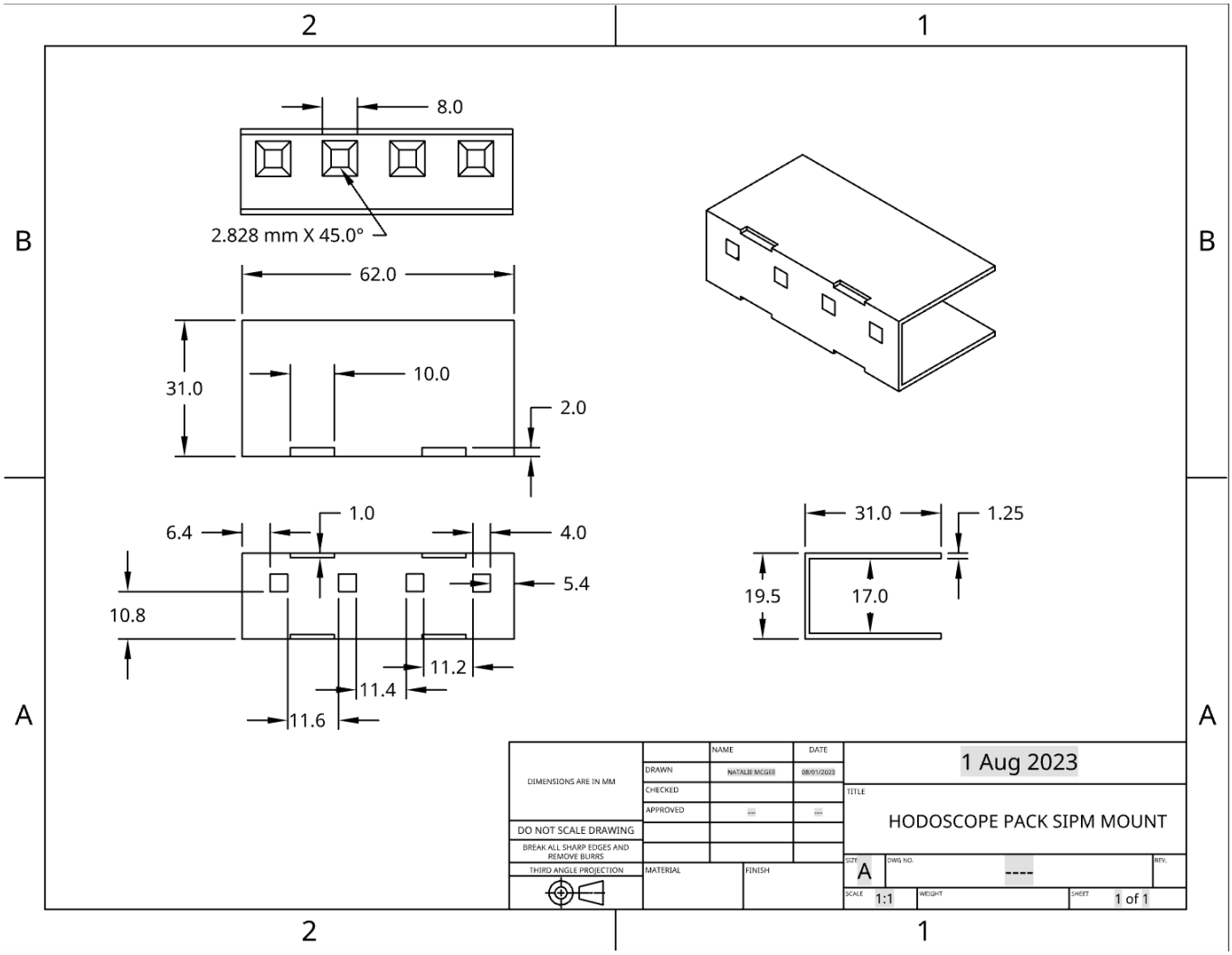

FIG. 17. Technical drawing of SiPM mount.

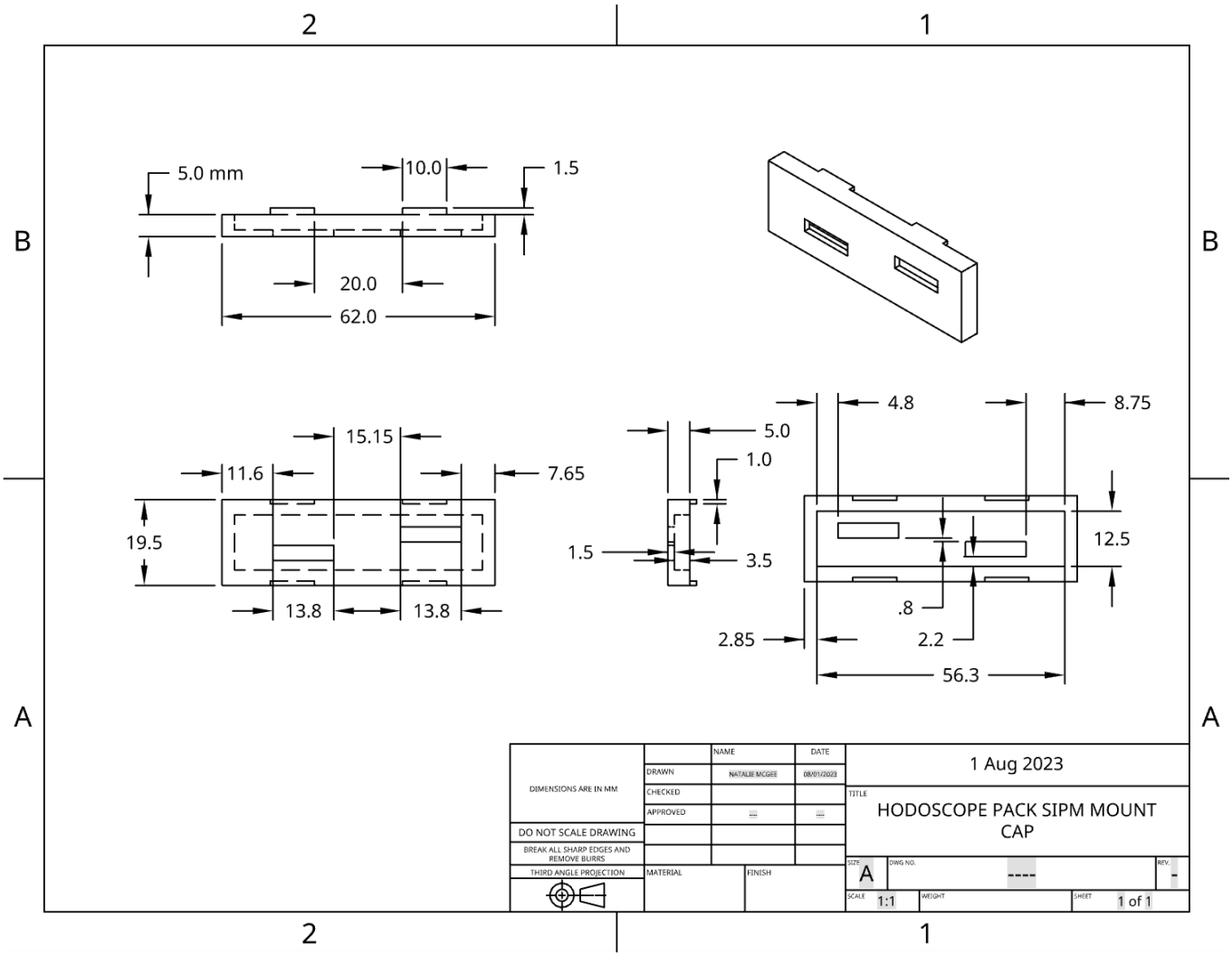

FIG. 18. Technical drawing of SiPM mount cap.

Appendix C: Scripts and Data Analysis

Code Listing 1. Micropython script used to program a Pico to measure pulse width data using PIO. Measurements are stored in the Pico as a CSV file. Script can be sent to Pico using Thonny, which can also be used to access the CSV file when written.

```
import time
from machine import Pin
import rp2
from rp2 import PIO, StateMachine, asm_pio # for PIO readout

total_events = 4000 #how many events to save
now = time.ticks_us()
filename = "hodoscope_read{}.csv".format(now)

@rp2.asm_pio(set_init=(rp2.PIO.IN_LOW), fifo_join = PIO.JOIN_RX) #initialize PIO. Set all pins low.
#fifo_join means we will be collecting 8 bits (joining 2 FIFO storage locations)

def reader():
    wrap_target() #Return here
    label("wait") #Waiting stage: waiting for trigger pin to go high
    jmp(pin, "setx") #When trigger pin goes high, go to setx stage
    jmp("wait") #If trigger pin is not high, go back to wait
    label("setx") #Setx stage: set the number of read iterations
    set(x, 7) #Set the counter x to 7
    label("read") #Read stage: read all GPIO pins together and repeat 8 times
    in_(pins, 32) #Read all 32 GPIO pins as digits of a word
    push() #Save the word to the FIFO
    jmp(x_dec, "read") #If counter==0, continue to stall. Else decrement x by 1 and return to read
    label("stall") #Stall stage: if trigger is still high, do not trigger again
    jmp(pin, "stall") #If trigger pin is still high, return to stall
    wrap() #Return to wrap target


sm0 = rp2.StateMachine(0, reader, freq=10000000, in_shiftdir=rp2.PIO.SHIFT_RIGHT, set_base=Pin(0),
                                                 jmp_pin = Pin(0))

#Set up state machine. 2nd argument is the function it calls, frequency is the frequency it
                                                 executes individual commands (in Hz),
#set_base=which pin to start counting from, jmp_pin = trigger pin
#Frequency of 10,000,000 Hz should give 100ns between commands. 4 commands in "read" means reads
                                                 occur every 400 ns
#This should give 400ns resolution for pulses up to 3200ns.

def decimalToBinary(n):
    # converting decimal to binary
    # and removing the prefix(0b)
    return bin(n).replace("0b", "")

def getdata(): #this function gets the words from the FIFO
    global eventnum
    result1 = str(decimalToBinary(sm0.get())) + "," #it will stall here until there is info in FIFO
    time1 = str(time.ticks_us()) + "," #timestamp
    result2 = str(decimalToBinary(sm0.get())) + "," #record the individual words as strings
    result3 = str(decimalToBinary(sm0.get())) + ","
    result4 = str(decimalToBinary(sm0.get())) + ","
    result5 = str(decimalToBinary(sm0.get())) + ","
    result6 = str(decimalToBinary(sm0.get())) + ","
    result7 = str(decimalToBinary(sm0.get())) + ","
    result8 = str(decimalToBinary(sm0.get())) + ","
    time2 = str(time.ticks_us()) #timestamp
    data = str(eventnum)+','+time1+result1+result2+result3+result4+result5+result6+result7+result8+
                                                    time2
    file.write(data+"\n")
    print("Events Saved: " + str(eventnum) + " of " + str(total_events))
```

```
sm0.active(1) #activate PIO state machine
eventnum = 0

with open(filename, 'w') as file:
    while eventnum<=total_events: #save a certain number of events
        getdata()
        eventnum+=1

print(filename +" saved to Pico")
```

Code Listing 2. Python script used to analyze PIO pulse measurement data saved as CSV file. Depending on the arguments passed, it will return data organized by event and by pin (Figure 19)

```
import ast
import csv
import sys

filename = sys.argv[1]
pins = ast.literal_eval(sys.argv[2])
pin_lists = [[] for _ in pins] #make a list of sublists each sublist corresponding to the values of
                                                    one pin during an event

count = 0 #number of coincident events

with open(filename, newline=None, encoding='utf-8') as file:
    reader = csv.reader(file, delimiter=',')

    for row in reader:                              #each row corresponds to a single event (8 words)
        for i in range(len(pins)):
            pin_lists[i] = [int(row[2][-pins[i]-1])] #populate sublists with pin values for this
                                                                event
            pin_lists[i].append(int(row[3][-pins[i]-1]))
            pin_lists[i].append(int(row[4][-pins[i]-1]))
            pin_lists[i].append(int(row[5][-pins[i]-1]))
            pin_lists[i].append(int(row[6][-pins[i]-1]))
            pin_lists[i].append(int(row[7][-pins[i]-1]))
            pin_lists[i].append(int(row[8][-pins[i]-1]))
            pin_lists[i].append(int(row[9][-pins[i]-1]))

        first_nums = [pin_list[0] for pin_list in pin_lists] #initial values of each pin for this
                                                              event
        coincidence = False
        if first_nums.count(1) > 1:
             coincidence = True                         #multiple pins are "on" @first timestamp

        if sys.argv[3] == "and" and coincidence:        #if argument "and" is passed (coincidence)
            count += 1
            print("Event Number " + row[0] + ": Timestamp = " + row[1])
            print("Coincident count = " + str(count) + str(count1))
            for i in range(len(pins)):
                if pin_lists[i].count(1) > 2:
                    large = "LARGE?"
                else:
                    large = ""
                print("Pin {num}".format(num=pins[i]) + str(pin_lists[i][1:]) + large)


        if sys.argv[3] != "and":                        #if argument "or" is passed (all events)
            print("Event Number " + row[0] + ": Timestamp = " + row[1])
            for i in range(len(pins)):
                if pin_lists[i].count(1) > 2:
                    large = "LARGE?"
                else:
                    large = ""
                print("Pin {num}".format(num=pins[i]) + str(pin_lists[i][1:]) + large)
```

```
Event Number 2668: Timestamp = 952558165
Coincident count = 2660
Pin 1[1, 1, 1, 1, 1, 1, 1]LARGE?
Pin 2[1, 1, 1, 1, 1, 1, 1]LARGE?
Pin 3[1, 1, 1, 1, 1, 1, 1]LARGE?
Pin 4[0, 0, 0, 0, 0, 0, 0]
Pin 5[0, 0, 0, 0, 0, 0, 0]
Pin 6[0, 0, 0, 0, 0, 0, 0]
Pin 7[0, 0, 0, 0, 0, 0, 0]
Event Number 2671: Timestamp = 953133288
Coincident count = 2670
Pin 1[0, 1, 1, 1, 1, 1, 1]LARGE?
Pin 2[1, 1, 1, 1, 1, 1, 1]LARGE?
Pin 3[1, 1, 1, 1, 1, 1, 1]LARGE?
Pin 4[0, 0, 0, 0, 0, 0, 0]
Pin 5[0, 0, 0, 0, 0, 0, 0]
Pin 6[0, 0, 0, 0, 0, 0, 0]
Pin 7[0, 0, 0, 0, 0, 0, 0]
Event Number 2691: Timestamp = 965341335
Coincident count = 2680
Pin 1[0, 0, 0, 0, 0, 0, 0]
Pin 2[0, 0, 0, 0, 0, 0, 0]
Pin 3[1, 1, 1, 1, 1, 1, 1]LARGE?
Pin 4[0, 0, 0, 1, 1, 1, 1]LARGE?
Pin 5[0, 0, 0, 0, 0, 0, 0]
Pin 6[0, 0, 0, 0, 0, 0, 0]
Pin 7[1, 0, 1, 1, 1, 1, 1]LARGE?
Event Number 2712: Timestamp = 977715238
Coincident count = 2690
Pin 1[0, 0, 0, 0, 0, 0, 0]
Pin 2[1, 1, 1, 1, 1, 1, 1]LARGE?
Pin 3[1, 1, 1, 1, 1, 1, 1]LARGE?
Pin 4[0, 0, 0, 0, 0, 0, 0]
Pin 5[0, 0, 0, 0, 0, 0, 0]
Pin 6[0, 0, 0, 0, 0, 0, 0]
Pin 7[0, 0, 0, 0, 0, 0, 0]
Event Number 2713: Timestamp = 977930754
Coincident count = 2700
Pin 1[0, 0, 0, 0, 0, 0, 0]
Pin 2[0, 0, 0, 0, 0, 0, 0]
Pin 3[1, 1, 1, 1, 0, 0, 0]LARGE?
Pin 4[0, 0, 0, 0, 0, 0, 0]
Pin 5[0, 0, 0, 0, 0, 0, 0]
Pin 6[1, 1, 1, 1, 1, 1, 1]LARGE?
Pin 7[0, 0, 0, 0, 0, 0, 0]
```

FIG. 19. Example output from PIO analysis script